Journal of Sensor Science and Technology
Vol. 33, No. 5 (2024) pp. 366-372
http://dx.doi.org/10.46670/JSST.2024.33.5.366
pISSN 1225-5475/eISSN 2093-7563

Enhanced Electrochemical Detection of Heavy Metal Ions *via* Post-synthetic Schiff Base Modification of MWCNT-MOF Composites

Yeon-Joo Kim[1], Seung-Ho Choi[1], and Seon-Jin Choi[1,+]

Abstract

In this study, we present a novel approach to improve electrochemical heavy metal ion (HMI) sensing responses *via* post-synthetic modification of carbon nanotube-based metal-organic framework (MOF) nanocomposites with a Schiff base. UiO66-NH_2 was employed as the MOF and incorporated with multi-walled carbon nanotubes (MWCNT) through *in-situ* growth, enhancing the electrical conductivity of the MWCNT-UiO66-NH_2 composite. Subsequently, the Schiff base, which has been proven to be an excellent ligand for metal ion detection, was functionalized onto MWCNT-UiO66-NH_2 *via* post-synthetic modification to improve its HMI absorption capacity. To evaluate the effect of the Schiff base on HMI detection capacity, electrochemical sensing of Cd^{2+}, Pb^{2+}, Cu^{2+}, and Hg^{2+} was performed in an aqueous solution utilizing the MWCNT-UiO66-Schiff modified electrode as well as the bare electrode. Individual differential pulse anodic stripping voltammetry results revealed that the modified electrode with MWCNT-UiO66-Schiff exhibited increased HMI sensing properties, especially with 1.82-fold improvement in average oxidation currents toward 10 μM of Cu^{2+} compared to that for a bare glassy carbon electrode. The selective Cu^{2+}-sensing properties of MWCNT-UiO66-Schiff were reflected in the highly selective Cu^{2}-binding affinity of the Schiff base-containing model molecules compared to those of Cd^{2+}, Hg^{2+}, and Pb^{2+}. Our work provides a new strategy for improving the sensing properties of electrochemical HMI sensors by the post-synthetic modification of MWCNT-UiO66 with a Schiff base.

Keywords: Schiff base, Multi-walled carbon nanotubes, Metal-organic framework, Post-synthetic modification, Heavy metal ions, Electrochemical sensor

1. INTRODUCTION

Heavy metal ions (HMIs) are highly hazardous water pollutants and pose a serious threat to human health and aquatic ecosystems [1,2]. HMIs are non-degradable in water and can accumulate in the human body through the ingestion of contaminated water or the food chain [3]. Therefore, many analytical techniques have been developed for their detection in water [4-7]. Among the available analytical technologies, spectroscopic methods can accurately determine HMI concentrations with low detection limits [8-10]. However, these methods require complex analytical procedures, are expensive, and have low portability. Therefore, there is a high demand for alternative technologies that are efficient and suitable for on-site HMI detection.

To address these issues, electrochemical methods, which offer rapid analysis, simple operation, and cost-effectiveness, have been proposed [11-14]. Among these methods, differential pulse anodic stripping voltammetry (DPASV) is a widely used method for HMI detection at low concentrations, providing high selectivity, fast screening rate, and excellent sensitivity [15-17].

Metal-organic frameworks (MOFs) are promising sensing materials for HMI absorption because of their large surface area, high porosity, and excellent chemical stability [18-21]. Post-synthetic modifications can further enhance the HMI absorption properties through the functionalization of organic ligands on MOFs. Schiff base groups, which contain nitrogen and oxygen donor atoms, are the ligands that serve as outstanding metal chelators as they can stabilize metal ions by forming metal complexes [22,23]. Therefore, Schiff bases have been functionalized on MOFs to maximize their metal ion absorption capacity [24,25]. Thus, the electrochemical sensing properties of MOFs can be improved by functionalization with Schiff bases. However, the applications of MOFs as electrical insulators in electrochemical sensors are limited. To increase electrical

[1]Division of Materials Science and Engineering, Hanyang University
222 Wangsimni-ro, Seongdong-gu, Seoul 04763, Republic of Korea
[+]Corresponding author: sjchoi27@hanyang.ac.kr
(Received: Sep. 2, 2024, Revised: Sep. 11, 2024, Accepted: Sep. 20, 2024)

conductivity, carbon nanotubes (CNTs) are frequently incorporated into MOFs to facilitate ion transport in aqueous electrolytes [26-28].

The incorporation of MOFs into CNTs can be achieved by *in-situ* and *ex-situ* approaches [29]. In the *in-situ* approach, MOF particles are directly grown on multi-walled CNTs (MWCNTs) and chemically integrated with acid-activated MWCNT surfaces [30,31]. This chemical interaction between MOFs and CNTs exhibits strong binding compared to the *ex-situ* strategy relying on physical interaction such as hydrogen bonding and π–π stacking [32].

In this paper, we report the improved HMI detection capability of an electrochemical sensor using a MWCNT-UiO66 composite functionalized with a Schiff base (MWCNT-UiO66-Schiff). We used UiO66-NH_2, which contains amine groups, as the MOF template for MWCNT-MOF to increase the density of the Schiff base functional groups on the electrode. A comparative HMI-binding study of the Schiff base-containing model molecule was conducted to investigate the effect of the Schiff base group on the selective HMI absorption affinity among various HMIs, such as Cd^{2+}, Pb^{2+}, Cu^{2+}, and Hg^{2+}. The selective and sensitive Cu^{2+} detection capabilities of the electrodes modified with the MWCNT-UiO66-Schiff composite were investigated *via* simultaneous and individual DPASV analyses and the results were compared with those obtained using bare electrodes.

2. EXPERIMENTAL

2.1 Materials

All chemicals and reagents were used as received without further purification. Carboxylic acid-functionalized multi-walled carbon nanotube (MWCNT-COOH), zirconium chloride, 2-aminoterephthalic acid (NH_2-BDC), salicylaldehyde, aniline, anhydrous methanol (MeOH, 99.8%), and monobasic and dibasic potassium phosphate were purchased from Sigma-Aldrich. *N, N*-dimethylformamide (DMF, 99.5%) and dimethyl sulfoxide (DMSO) were purchased from Daejung Chemical & Materials. Ethanol (EtOH, 99.5%), acetone (99.7%), and hydrochloric acid (HCl, 35–37%) were purchased from Samchun Chemical Co., Ltd.

2.2 Synthesis of MWCNT-UiO66-NH_2

MWCNT-UiO66-NH_2 was synthesized through *in-situ* growth of UiO66-NH_2 on the surface of MWCNTs using solvothermal synthesis. During this process, the UiO66-NH_2 crystals were nucleated and grown on the acid-activated surface of the MWCNTs. MWCNT-COOH (30 mg) was dispersed in DMF (100 mL) *via* sonication for 1 h to obtain a homogeneous MWCNT-COOH dispersion. Subsequently, 1.1 mmol of zirconium chloride and 1.0 mmol of NH_2-BDC were dissolved in the MWCNT dispersion. After stirring for 30 min at 85°C, the mixture was autoclaved and heated to 120°C in a furnace for 24 h. After cooling to room temperature, the product solution was washed with DMF to remove unreacted UiO66-NH_2 precursors and centrifuged at 4,500 rpm for 10 min. The precipitate was washed with acetone for solvent exchange from the pores of UiO66-NH_2 and centrifuged. The precipitates were dried under vacuum at 60°C overnight and ground in a mortar to obtain MWCNT-UiO66-NH_2.

2.3 Synthesis of MWCNT-UiO66-Schiff

Schiff base functionalization was performed on MWCNT-UiO66-NH_2 using salicylaldehyde molecule *via* condensation reaction, producing MWCNT-UiO66-Schiff (Fig. 1). Specifically, 50 mg MWCNT-UiO66-NH_2 was dispersed in EtOH (12 mL) *via* sonication for 1 h to obtain a homogenous MWCNT-UiO66-NH_2 dispersion. Subsequently, 2.56 mmol salicylaldehyde was added to the dispersion and refluxed for 24 h. After the reaction, the mixture was poured into 100 mL EtOH to dissolve the unreacted salicylaldehyde. After being stirred overnight, the diluted mixture was dispersed by sonication for 30 min and centrifuged to obtain supernatants containing the products. The supernatants were filtered, washed with EtOH several times, and dried at 60°C in a vacuum. The resulting black powder was obtained using the grinding procedure described above.

2.4 Electrochemical measurement

2.4.1 Modification of GCE

Before modification, a glassy carbon electrode (GCE) was polished on a polishing pad with an alumina slurry and rinsed with

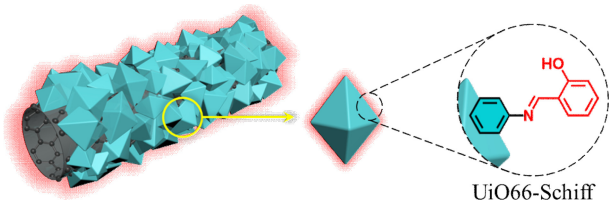

Fig. 1. Schematic illustration of MWCNT-UiO66-Schiff.

distilled water. The MWCNT-UiO66-NH_2 and MWCNT-UiO66-Schiff composites were dispersed in MeOH using a sonication bath for 1 h, resulting in 1 mg/mL of homogeneous dispersion. Of this dispersion, 2 μL was drop-coated on the polished GCE. Subsequently, the modified GCE was dried under vacuum to evaporate MeOH.

2.4.2 DPASV sensing measurement

The modified GCE was used as the working electrode in a 3-electrode system with a Pt wire as the counter electrode and Ag/AgCl as the reference electrode. The three electrodes were immersed in an electrochemical cell containing 10 mL of a 1.0 M potassium phosphate buffer solution (pH 7.0) as the electrolyte, into which the HMI solutions were injected. The HMI stock solutions (10^{-1} μM) were prepared by dissolving the nitrate- or chloride-based metal salts in DI water. HCl was added to achieve a concentration of 10^{-1} μM for pH 2, thereby obtaining a metal-soluble stock solution.

The DPASV measurement was performed in three steps: deposition (at 1.0 V, 300 s), stripping (potential range from –1.0 V to 0.6 V), and cleaning (at 1.0 V, 600 s) with a scan rate of 5 mV/s, an amplitude of 50 mV, and a pulse width of 50 msec. Before each deposition step, the electrolyte containing the HMI stock solution was stirred for 1 min to evenly distribute the HMIs. The DPASV sensing properties of MWCNT-UiO66-Schiff modified GCE toward HMIs were evaluated in comparison with those obtained with the bare GCE, thereby revealing the influence of MWCNT-UiO66-Schiff on HMI detection.

3. RESULTS AND DISCUSSION

3.1 Morphology and structure of MWCNT-UiO66-Schiff

The morphologies of MWCNT-COOH, UiO66-NH_2, MWCNT-UiO66-NH_2, and MWCNT-UiO66-Schiff were examined by scanning electron microscopy (SEM) (Fig. 2). The SEM image of MWCNT-COOH exhibited a stem-like structure (average diameter 20 nm) (Fig. 2 (a)), whereas that of the UiO66-NH_2 particles exhibited an octahedral nanocrystal structure (average diameter 150 nm) (Fig. 2 (b)). The UiO66-NH_2 particles were decorated on the surface of MWCNT-COOH by the *in-situ* growth (Fig. 2 (c)). The morphology of the chemically modified MWCNT-UiO66-Schiff composite was maintained after the post-synthetic modification, similar to that of MWCNT-UiO66-NH_2

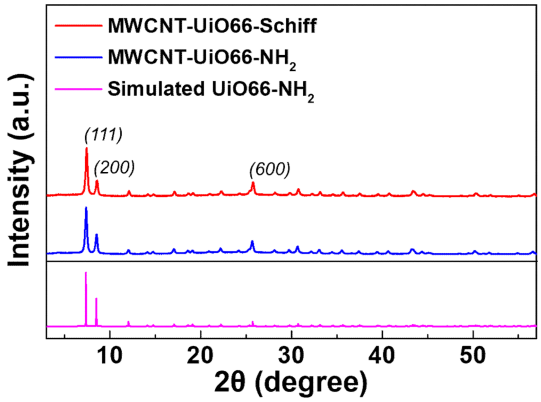

Fig. 2. XRD patterns of MWCNT-UiO66-Schiff, MWCNT-UiO66-NH_2, and simulated UiO66-NH_2.

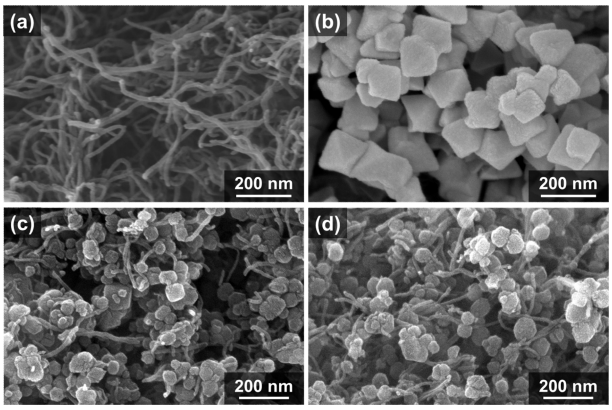

Fig. 3. SEM images of (a) MWCNT-COOH, (b) UiO66-NH_2, (c) MWCNT-UiO66-NH_2, and (d) MWCNT-UiO66-Schiff.

(Fig. 2 (d)). Based on these results, we confirmed that the carboxylic acid groups acted as nucleation sites for the growth of the UiO66-NH_2 crystals and maintained their structure after chemical treatment. In addition, no significant changes in morphology were observed for MWCNT-UiO66-Schiff after Schiff base functionalization.

The X-ray diffraction (XRD) patterns of MWCNT-UiO66-Schiff, MWCNT-UiO66-NH_2, and simulated UiO66-NH_2 are displayed in Fig. 3. The XRD peaks of the *in-situ* grown MWCNT-UiO66-NH_2 were well matched with those of simulated UiO66-NH_2, especially at 2θ = 7.25° (111), 8.68° (200), and 25.7° (600). These results indicate that UiO66-NH_2 particles were successfully formed on the surface of MWCNT-COOH *via* solvothermal synthesis. After the post-synthetic modification with salicylaldehyde, the XRD peaks of MWCNT-UiO66-Schiff were consistent with those of MWCNT-UiO66-NH_2, indicating that crystallinity was preserved after the Schiff base functionalization of UiO66-NH_2.

Attenuated total reflection-Fourier transform infrared (ATR-FTIR) analysis was performed to confirm Schiff base

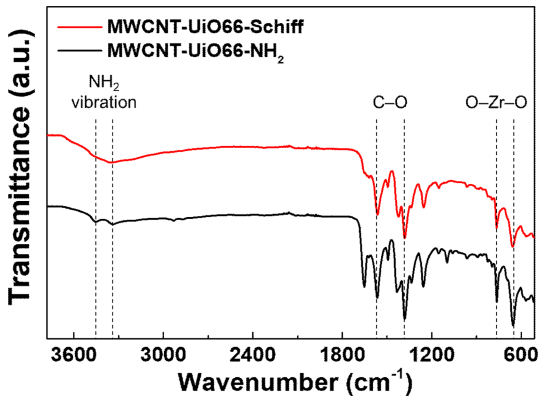

Fig. 4. ATR-FTIR spectra of MWCNT-UiO66-Schiff and MWCNT-UiO66-NH_2.

functionalization of the surface of MWCNT-UiO66-NH_2 (Fig. 4). The NH_2 vibration peaks of the amine group of NH_2-BDC were observed in the FTIR spectra of MWCNT-UiO66-NH_2 at 3338 cm^{-1} and 3454 cm^{-1} [33]. In contrast to MWCNT-UiO66-NH_2, the NH_2-related peaks disappeared in the spectrum of MWCNT-UiO66-Schiff, which was attributed to the formation of a Schiff base by the reaction with the amine group during post-synthetic modification [34,35]. Furthermore, the O–Zr–O stretching peaks originating from the $[Zr_6O_4(OH)_4]^{12+}$ secondary building unit of UiO66-NH_2 were confirmed at 657 and 765 cm^{-1} in the FTIR spectra of MWCNT-UiO66-NH_2 and MWCNT-UiO66-Schiff [36, 37]. The C–O peaks of NH_2-BDC were observed at 1382 and 1564 cm^{-1} [36,37]. The peaks originating from the O–Zr–O and C–O bonds after the *in-situ* synthesis and post-synthetic modification indicated the structural and chemical stabilities of the MWCNT-UiO66-NH_2 and MWCNT-UiO66-Schiff composites.

3.2 HMI binding study of Schiff base model molecule

UV-vis spectroscopy was used to evaluate the HMI-binding properties of the Schiff base toward HMIs. To conduct UV-vis titration, a model molecule of MWCNT-UiO66-Schiff was synthesized by a condensation reaction (Fig. 5 (a)). To analyze the chemical interaction between the Schiff base and HMI, we used aniline, which has a structure derived from NH_2-BDC except for the two carboxylic acid groups, for model molecule synthesis. Specifically, 1 mmol aniline and 1 mmol salicylaldehyde were added to MeOH, and the mixture was refluxed for 12 h. After the reaction, MeOH in the resulting solution was evaporated using a rotary evaporator. The product was further dried at 60°C in vacuum overnight to obtain yellow precipitates (ANS).

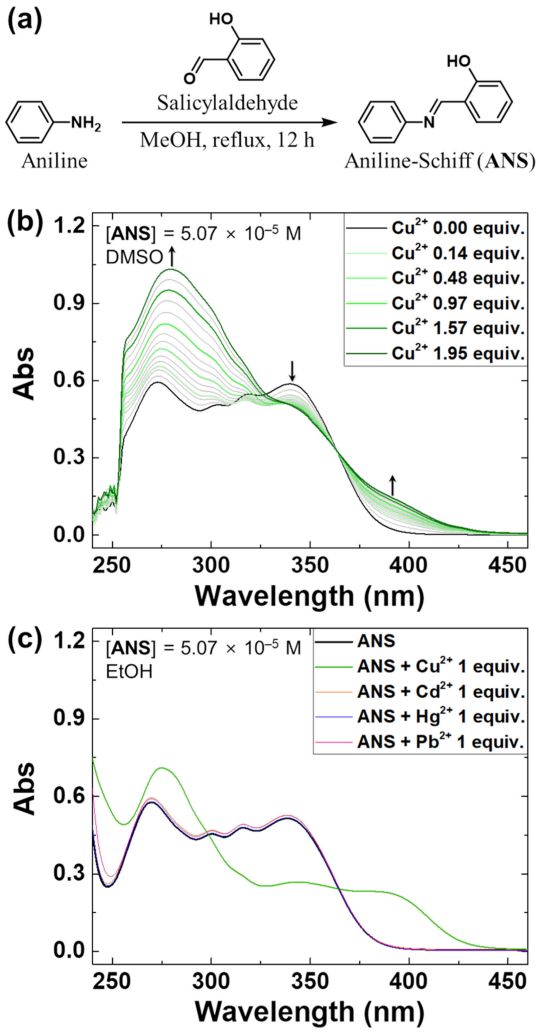

Fig. 5. (a) Synthesis of ANS by condensation reaction between aniline and salicylaldehyde. (b) UV-vis titration of ANS toward Cu^{2+} in DMSO. (c) UV-vis absorbance transitions of ANS with addition of 1 equivalent each of Cu^{2+}, Cd^{2+}, Hg^{2+}, and Pb^{2+} in EtOH.

The HMI-binding properties of ANS toward various HMIs such as Cu^{2+}, Cd^{2+}, Hg^{2+}, and Pb^{2+} were investigated using UV-vis spectroscopy (Fig. 5 (b) and (c)). UV-vis titrations were performed by adding Cu^{2+} to a 3 mL DMSO-filled cuvette cell containing 5.07×10^{-5} M ANS (Fig. 5 (b)). With the addition of Cu^{2+}, the UV-vis absorbance band of ANS gradually increased at 297 and 389 nm and decreased at 340 nm, with isosbestic points at 364 and 328 nm. To further investigate the selective binding properties of ANS, 1 equivalent each of Cu^{2+}, Cd^{2+}, Hg^{2+}, and Pb^{2+} was added to an EtOH solution containing 5.07×10^{-5} M ANS (Fig. 5 (c)). Among the HMIs, significant absorbance transitions were observed for Cu^{2+}, whereas negligible absorbance transitions were observed for Cd^{2+}, Hg^{2+}, and Pb^{2+}, indicating the selective Cu^{2+}-binding properties of ANS.

3.3 Electrochemical HMI sensing property

3.3.1 Simultaneous DPASV sensing property

The simultaneous sensing properties of MWCNT-UiO66-Schiff modified GCE and bare GCE were evaluated by measuring the oxidation peak currents toward the HMIs in the anodic stripping step (Fig. 6 (a)). The modified GCE with MWCNT-UiO66-Schiff exhibited improved oxidation currents toward 10 μM of Cd^{2+}, Pb^{2+}, Cu^{2+}, and Hg^{2+} compared to those observed with the bare GCE (Fig. 6 (b)). In particular, an additional oxidation peak at –0.2 V was observed for the bare GCE, attributed to the Pb–Cu overlapping oxidation peaks due to the formation of an intermetallic compound at the deposition site, leading to the degradation of the oxidation currents [38,39]. However, the mixed peak disappeared for the MWCNT-UiO66-Schiff modified GCE, indicating improved selective and sensitive Cu^{2+} detection capabilities. In addition, the MWCNT-UiO66-Schiff modified GCE exhibited a proportional increase in sensing responses with HMI concentrations increasing in the range of 0–10 μM (Fig. 6 (c)). These results indicate that the GCE modified with MWCNT-UiO66-Schiff exhibit enhanced HMI detection capability and improved selective Cu^{2+} sensing properties.

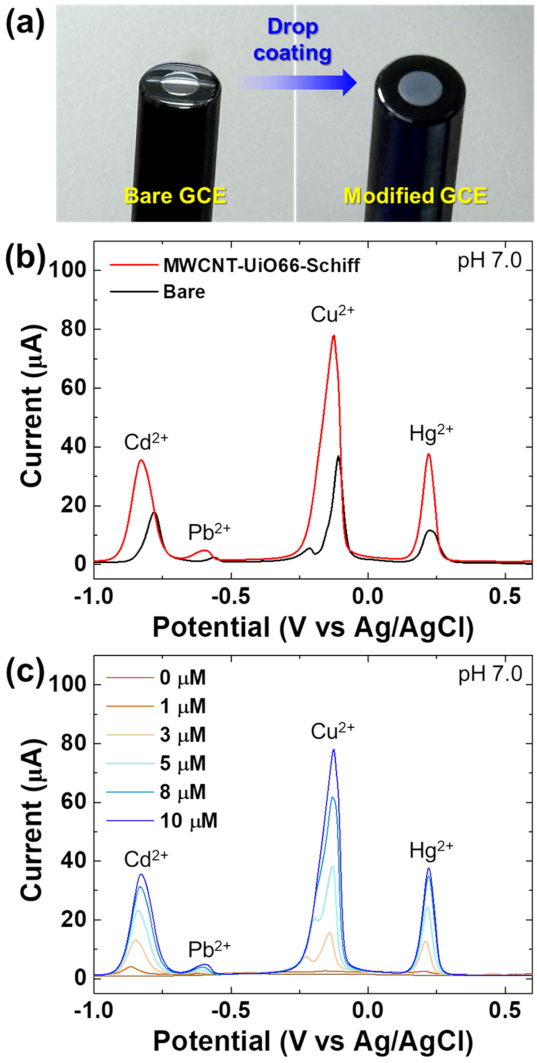

Fig. 6. (a) Optical images of the bare and modified GCEs. (b) Simultaneous DPASV curves of MWCNT-UiO66-Schiff modified GCE and bare GCE toward 10 μM of Cu^{2+}, Cd^{2+}, Hg^{2+}, and Pb^{2+}. (c) Simultaneous DPASV curves of MWCNT-UiO66-Schiff modified GCE with HMI concentrations increasing in the range of 0–10 μM.

3.3.2 Individual DPASV sensing property

To further investigate the effect of the Schiff base on the HMI sensing properties, the individual DPASV sensing properties of the MWCNT-UiO66-Schiff modified GCE were investigated under identical DPASV sensing conditions with simultaneous sensing characterization. Table 1 displays the improvement in oxidation current value toward 10 μM of HMI after individual DPASV sensing evaluation using MWCNT-UiO66-Schiff modified GCE and bare GCE. The MWCNT-UiO66-Schiff modified GCE exhibited an improved sensing response toward Cd^{2+}, Pb^{2+}, Cu^{2+}, and Hg^{2+} compared to the bare GCE. Notably, the average oxidation current improvement (I/I_0) from the bare GCE to MWCNT-UiO66-Schiff modified GCE was the highest for Cu^{2+}, a 1.82-fold improvement, followed by Cd^{2+}, Hg^{2+}, and Pb^{2+}. The selective oxidation current improvement for the MWCNT-UiO66-Schiff modified GCE demonstrated highly selective responses toward Cu^{2+}, corresponding to the simultaneous sensing results. These improvements were attributed

Table 1. Individual oxidation current improvement for MWCNT-UiO66-Schiff modified GCE compared to that for bare GCE toward 10 μM of HMI.

Analyte HMI	GCE condition	Oxidation current (μA)	Improvement (I/I_0)*
Cd^{2+}	Bare	23.64	1.78
	Modified	41.98	
Pb^{2+}	Bare	0.55	1.31
	Modified	0.72	
Cu^{2+}	Bare	10.34	1.82
	Modified	18.80	
Hg^{2+}	Bare	9.52	1.32
	Modified	12.52	

*I/I_0: Oxidation peak current improvement for modified GCE (I: oxidation peak current of modified GCE, I_0: oxidation peak current of bare GCE)

to the strong interaction between Cu^{2+} and the Schiff base molecules. The simultaneous and individual DPASV results of MWCNT-UiO66-Schiff modified GCE were in good agreement with the HMI-binding study of ANS confirmed by UV-vis titrations.

4. CONCLUSIONS

In summary, we developed an electrochemical HMI sensor by modifying a GCE using a Schiff base-functionalized MWCNT-UiO66 composite. MWCNT-UiO66-Schiff composites were synthesized *via* the post-synthetic modification using salicylaldehyde on the MWCNT-UiO66-NH_2. The functionalization of the Schiff base on MWCNT-UiO66-NH_2 was confirmed by SEM, XRD, and ATR-FTIR analyses. The HMI-binding properties of **ANS**, the model molecule of MWCNT-UiO66-Schiff, were investigated by UV-vis spectroscopy, revealing the selective Cu^{2+}-binding affinity of **ANS**. This result was consistent with the DPASV sensing result of MWCNT-UiO66-Schiff modified GCE, showing a 1.82-fold improvement in individual oxidation current compared to that with the bare GCE. In addition, we confirmed that the MWCNT-UiO66-Schiff modified GCE expands the HMI deposition sites, reducing the competitive deposition of Cu^{2+} and Hg^{2+} in simultaneous HMI sensing measurements. This work paves the way for an electrochemical HMI sensor *via* post-synthetic modification of MWCNT-UiO66 composites using a Schiff base, providing real-time and on-site HMI detection capabilities.

ACKNOWLEDGMENT

This work was supported by the National Research Foundation of Korea (NRF) grant funded by the Korean Government (MSIT) (No. RS-2023-00236572 and RS-2024-00407282). This work was also supported by the U.S. Army Combat Capabilities Development Command Soldier Center (DEVCOM SC) and the International Technology Center Pacific (ITC-PAC) Global Research Project under contract FA520922C0008 and conducted at Hanyang University. This research was supported by the Brain Korea 21 Fostering Outstanding Universities for Research (BK21 FOUR) project of the National Research Foundation of Korea Grant.

REFERENCES

[1] R. McRae, P. Bagchi, S. Sumalekshmy, and C. J. Fahrni, "In situ imaging of metals in cells and tissues", *Chem. Rev.*, Vol. 109, No. 10, pp. 4780-4827, 2009.

[2] E. L. Que, D. W. Domaille, and C. J. Chang, "Metals in neurobiology: probing their chemistry and biology with molecular imaging", *Chem. Rev.*, Vo. 108, No. 5, pp. 1517-1549, 2008.

[3] L. A. Malik, A. Bashir, A. Qureashi, and A. H. Pandith, "Detection and removal of heavy metal ions: a review", *Environ. Chem. Lett.*, Vol. 17, No. 4, pp. 1495-1521, 2019.

[4] D. T. Quang and J. S. Kim, "Fluoro-and chromogenic chemodosimeters for heavy metal ion detection in solution and biospecimens", *Chem. Rev.*, Vol. 110, No. 10, pp. 6280-6301, 2010.

[5] D. W. Domaille, E. L. Que, and C. J. Chang, "Synthetic fluorescent sensors for studying the cell biology of metals", *Nat. Chem. Biol.*, Vol. 4, No. 3, pp. 168-175, 2008.

[6] D. W. Domaille, L. Zeng, and C. J. Chang, "Visualizing ascorbate-triggered release of labile copper within living cells using a ratiometric fluorescent sensor", *J. Am. Chem. Soc.*, Vol. 132, No. 4, pp. 1194-1195, 2010.

[7] C. Bargossi, M. C. Fiorini, M. Montalti, L. Prodi, and N. Zaccheroni, "Recent developments in transition metal ion detection by luminescent chemosensors", *Coord. Chem. Rev.*, Vol. 208, No. 1, pp. 17-32, 2000.

[8] V. N. Losev, O. V. Buyko, A. K. Trofimchuk, and O. N. Zuy, "Silica sequentially modified with polyhexamethylene guanidine and Arsenazo I for preconcentration and ICP–OES determination of metals in natural waters", *Microchem. J.*, Vol. 123, pp. 84-89, 2015.

[9] X. Yuan, K. H. Ling, and C. W. Keung, "The analysis of heavy metals in Chinese herbal medicine by flow injection–mercury hydride system and graphite furnace atomic absorption spectrometry", *Phytochem. Anal.*, Vol. 20, No. 4, pp. 293-297, 2009.

[10] F. Yarur, J.-R. Macairan, and R. Naccache, "Ratiometric detection of heavy metal ions using fluorescent carbon dots", *Environ. Sci. Nano.*, Vol. 6, No. 4, pp. 1121-1130, 2019.

[11] G. Aragay and A. Merkoci, "Nanomaterials application in electrochemical detection of heavy metals", *Electrochim. Acta.*, Vol. 84, pp. 49-61, 2012.

[12] L. Pujol, D. Evrard, K. Groenen-Serrano, M. Freyssinier, A. Ruffien-Cizsak, and P. Gros, "Electrochemical sensors and devices for heavy metals assay in water: the French groups' contribution", *Front. Chem.*, Vol. 2, p. 19, 2014.

[13] M. B. Gumpu, S. Sethuraman, U. M. Krishnan, and J. B. B. Rayappan, "A review on detection of heavy metal ions in water–an electrochemical approach", *Sens. Actuators B Chem.*, Vol. 213, pp. 515-533, 2015.

[14] A. Sbartai, P. Namour, A. Errachid, J. Krejči, R. Šejnohová, L. Renaud, M. Larbi Hamlaoui, A.-S. Loir, F. Garrelie, and C. Donnet, "Electrochemical boron-doped diamond film microcells micromachined with femtosecond laser: application to the determination of water framework directive metals", *Anal. Chem.*, Vol. 84, No. 11, pp. 4805-4811, 2012.

[15] Q. Ding, C. Li, H. Wang, C. Xu, and H. Kuang, "Electrochemical detection of heavy metal ions in water", *Chem.*

Commun., Vol. 57, No. 59, pp. 7215-7231, 2021.
[16] Y. Lu, X. Liang, C. Niyungeko, J. Zhou, J. Xu, and G. Tian, "A review of the identification and detection of heavy metal ions in the environment by voltammetry", *Talanta*, Vol. 178, pp. 324-338, 2018.
[17] C. Huangfu, L. Fu, Y. Li, X. Li, H. Du, and J. Ye, "Sensitive Stripping Determination of Cadmium (II) and Lead (II) on Disposable Graphene Modified Screen?Printed Electrode", *Electroanalysis*, Vol. 25, No. 9, pp. 2238-2243, 2013.
[18] J. Wen, Y. Fang, and G. Zeng, "Progress and prospect of adsorptive removal of heavy metal ions from aqueous solution using metal–organic frameworks: a review of studies from the last decade", *Chemosphere*, Vol. 201, pp. 627-643, 2018.
[19] E. L. Wong, E. Chow, and J. J. Gooding, "The electrochemical detection of cadmium using surface-immobilized DNA", *Electrochem. Commun.*, Vol. 9, No. 4, pp. 845-849, 2007.
[20] W. S. Chai, J. Y. Cheun, P. S. Kumar, M. Mubashir, Z. Majeed, F. Banat, S.-H. Ho, and P. L. Show, "A review on conventional and novel materials towards heavy metal adsorption in wastewater treatment application", *J. Clean. Prod.*, Vol. 296, pp. 126589, 2021.
[21] C. Wang, X. Liu, N. K. Demir, J. P. Chen, and K. Li, "Applications of water stable metal–organic frameworks", *Chem. Soc. Rev.*, Vol. 45, No. 18, pp. 5107-5134, 2016.
[22] A. C. Ekennia, A. A. Osowole, L. O. Olasunkanmi, D. C. Onwudiwe, and E. E. Ebenso, "Coordination behaviours of new (bidentate N, O-chelating) Schiff bases towards copper (II) and nickel (II) metal ions: synthesis, characterization, antimicrobial, antioxidant, and DFT studies", *Res. Chem. Intermed.*, Vol. 43, pp. 3787-3811, 2017.
[23] Z. H. Chohan, A. Munawar, and C. T. Supuran, "Transition Metal Ion Complexes of Schiff?bases. Synthesis, Characterization and Antibacterial Properties", *Met. Based. Drugs.*, Vol. 8, No. 3, pp. 137-143, 2001.
[24] G. Yuan, Y. Tian, J. Liu, H. Tu, J. Liao, J. Yang, Y. Yang, D. Wang, and N. Liu, "Schiff base anchored on metal-organic framework for Co (II) removal from aqueous solution", *Chem. Eng. J.*, Vol. 326, pp. 691-699, 2017.
[25] M. Kaur, S. Kumar, M. Yusuf, J. Lee, R. J. Brown, K.-H. Kim, and A. K. Malik, "Post-synthetic modification of luminescent metal-organic frameworks using schiff base complexes for biological and chemical sensing", *Coord. Chem. Rev.*, Vol. 449, pp. 214214, 2021.
[26] X. Zhang, Y. Xu, and B. Ye, "An efficient electrochemical glucose sensor based on porous nickel-based metal organic framework/carbon nanotubes composite (Ni-MOF/CNTs)", *J. Alloys Compd.*, Vol. 767, pp. 651-656, 2018.
[27] H. Miyasaka, "Control of charge transfer in donor/acceptor metal–organic frameworks", *Acc. Chem. Res.*, Vol. 46, No. 2, pp. 248-257, 2013.
[28] X. Wan, H. Du, D. Tuo, X. Qi, T. Wang, J. Wu, and G. Li, "Uio-66/carboxylated multiwalled carbon nanotube composites for highly efficient and stable voltammetric sensors for gatifloxacin", *ACS Appl. Nano. Mater.*, Vol. 6, No. 20, pp. 19403-19413, 2023.
[29] X.-W. Liu, T.-J. Sun, J.-L. Hu, and S.-D. Wang, "Composites of metal–organic frameworks and carbon-based materials: preparations, functionalities and applications", *J. Mater. Chem. A.*, Vol. 4, No. 10, pp. 3584-3616, 2016.
[30] W. Liang, B. Wang, J. Cheng, D. Xiao, Z. Xie, and J. Zhao, "3D, eco-friendly metal-organic frameworks@ carbon nanotube aerogels composite materials for removal of pesticides in water", *J. Hazard. Mater.*, Vol. 401, p. 123718, 2021.
[31] L. Ge, Y. Yang, L. Wang, W. Zhou, R. De Marco, Z. Chen, J. Zou, and Z. Zhu, "High activity electrocatalysts from metal–organic framework-carbon nanotube templates for the oxygen reduction reaction", *Carbon.*, Vol. 82, pp. 417-424, 2015.
[32] D. D. Chronopoulos, H. Saini, I. Tantis, R. Zbořil, K. Jayaramulu, and M. Otyepka, "Carbon nanotube based metal–organic framework hybrids from fundamentals toward applications", *Small.*, Vol. 18, No. 4, p. 2104628, 2022.
[33] H. Saleem, U. Rafique, and R. P. Davies, "Investigations on post-synthetically modified UiO-66-NH2 for the adsorptive removal of heavy metal ions from aqueous solution", *Micropor. Mesopor. Mater.*, Vol. 221, pp. 238-244, 2016.
[34] S.-Y. Zhu and B. Yan, "A novel covalent post-synthetically modified MOF hybrid as a sensitive and selective fluorescent probe for Al^{3+} detection in aqueous media", *Dalton Trans.*, Vol. 47, No. 5, pp. 1674-1681, 2018.
[35] S. Wang, S. Hou, C. Wu, Y. Zhao, and X. Ma, "$RuCl_3$ anchored onto post-synthetic modification MIL-101 (Cr)-NH_2 as heterogeneous catalyst for hydrogenation of CO_2 to formic acid", *Chin. Chem. Lett.*, Vol. 30, No. 2, pp. 398-402, 2019.
[36] R. Chen, C.-a. Tao, Z. Zhang, X. Chen, Z. Liu, and J. Wang, "Layer-by-layer fabrication of core–shell Fe3O4@ UiO-66-NH2 with high catalytic reactivity toward the hydrolysis of chemical warfare agent simulants", *ACS Appl. Mater. Interfaces.*, Vol. 11, No. 46, pp. 43156-43165, 2019.
[37] J. H. Cavka, S. Jakobsen, U. Olsbye, N. Guillou, C. Lamberti, S. Bordiga, and K. P. Lillerud, "A new zirconium inorganic building brick forming metal organic frameworks with exceptional stability", *J. Am. Chem. Soc.*, Vol. 130, No. 42, pp. 13850-13851, 2008.
[38] X. Han, Z. Meng, H. Zhang, and J. Zheng, "Fullerene-based anodic stripping voltammetry for simultaneous determination of Hg (II), Cu (II), Pb (II) and Cd (II) in foodstuff", *Microchim. Acta.*, Vol. 185, pp. 1-9, 2018.
[39] P. Veerakumar, V. Veeramani, S.-M. Chen, R. Madhu, and S.-B. Liu, "Palladium nanoparticle incorporated porous activated carbon: electrochemical detection of toxic metal ions", *ACS Appl. Mater. Interfaces.*, Vol. 8, No. 2, pp. 1319-1326, 2016.